

# Aerodynamic Analysis of a Rigid Honeybee-Inspired Drone Using CFD and Static Simulation

Sahar Shaukat<sup>\*</sup>, Amash Rauf<sup>†</sup>

Email Correspondence\*: [saharshaukat2003@gmail.com](mailto:saharshaukat2003@gmail.com)

Institute of Space Technology, Islamabad, Pakistan.

## Abstract:

In the development of bio-inspired Micro Air Vehicles (MAVs), flapping-wing configurations derived from natural fliers such as honeybees offer unique advantages in maneuverability and stability within complex environments. However, modeling the unsteady aerodynamic behavior of flapping wings is computationally intensive. In this study, a simplified quasi-steady approach is adopted by simulating the aerodynamics of a rigid, honeybee-inspired drone at multiple static orientations using a virtual inflow rotation technique. Computational Fluid Dynamics (CFD) simulations are performed at various effective angles of attack by altering the direction of the incoming flow while keeping the wing geometry fixed. Key vortex structures, including leading-edge and wingtip vortices, are analyzed to evaluate their role in lift and thrust generation. Aerodynamic forces (lift, drag, and thrust) are quantified across multiple static orientations to gain insights into aerodynamic performance. In parallel, a basic static structural analysis of the rigid wing is conducted using the aerodynamic pressure loads obtained from the CFD simulations. The structural response under representative aerodynamic loads is evaluated to assess stress distribution and potential wing deformation. This combined aerodynamic and structural analysis provides a comprehensive understanding of wing performance and structural integrity, offering valuable data for optimizing bio-mimetic MAV design.

**Keywords:** Bio-Inspired Flight, Micro Air Vehicles (MAVs), Nano Air Vehicles (NAVs), Flapping Wing, Honeybee Kinematics, Unsteady Aerodynamics, Vortex Dynamics.

## 1. Introduction

Over the past two decades, advancements in the miniaturization of unmanned aerial systems have led to the emergence of Micro Air Vehicles (MAVs) and Nano Air Vehicles (NAVs), with an increasing focus on bio-inspired designs. Among these, flapping-wing MAVs, modeled after natural fliers such as birds and insects, offer exceptional agility and maneuverability, making them suitable for operations in confined or cluttered environments where traditional fixed-wing or rotary-wing platforms may be limited [3][1]. Honeybees (*Apis mellifera*) exhibit highly efficient flapping-wing flight mechanisms that involve complex unsteady aerodynamic phenomena, including dynamic stall, vortex shedding, and strong leading-edge vortex (LEV) stabilization, all of which contribute significantly to lift generation. However, fully capturing these unsteady effects in numerical simulations typically requires time-resolved computational methods, which can be computationally intensive [4]. This study adopts a simplified approach by discretizing the flapping cycle into multiple static orientations. The aerodynamic analysis is conducted by altering the direction of incoming airflow to simulate different phases of the flapping cycle using steady-state Computational Fluid Dynamics (CFD). Aerodynamic forces, pressure distributions, and vortex behaviors are analyzed at each static

<sup>\*</sup>Institute of Space Technology, Islamabad, Pakistan.

<sup>†</sup>Institute of Space Technology, Islamabad, Pakistan.

position. Subsequently, the pressure loads obtained from CFD are applied to the wing structure in a static structural simulation to evaluate stress distribution and potential deformation. This combined aerodynamic and structural analysis provides a comprehensive understanding of wing performance, contributing to the design optimization of flapping-wing MAVs.

## 2. Problem Statement

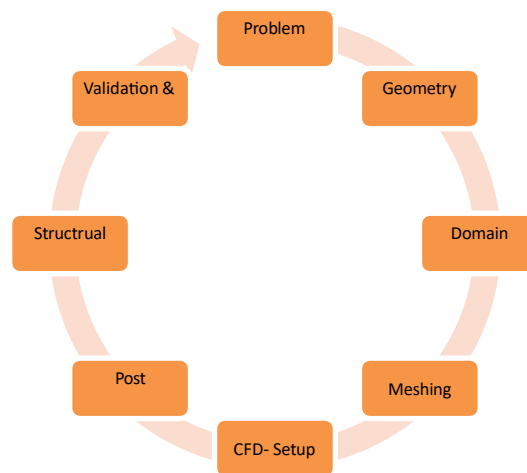
The unsteady aerodynamics of flapping wings, such as those observed in honeybee flight, involve complex phenomena including dynamic stall, vortex shedding, and rapidly changing flow separation. Accurately capturing these dynamics using time-dependent simulations is computationally demanding. To address this challenge, the present study simplifies flapping-wing motion into discrete static orientations by varying the inflow direction within a steady-state CFD framework. Additionally, structural integrity is a critical factor for MAV wings subjected to varying aerodynamic loads. Therefore, this study incorporates a basic static structural analysis to evaluate the wing's ability to withstand representative aerodynamic forces [5][1]. The combined aerodynamic and structural analysis aims to provide design insights that enhance wing performance while ensuring structural durability.

## 3. Objectives

- Simulate the aerodynamic performance of a rigid honeybee-inspired wing using steady-state CFD at multiple effective angles of attack through virtual inflow rotation.
- Analyze vortex dynamics, including leading-edge and wingtip vortices, to understand their influence on lift and drag generation [6][1].
- Quantify aerodynamic forces (lift, drag, thrust) at each simulated static position.
- Investigate flow separation patterns and pressure distributions across varying angles to assess aerodynamic efficiency.
- Validate simulation trends against available biological data to ensure the reliability of the static analysis approach [3].

## 4. Methodology

This study employs a combined computational approach involving Computational Fluid Dynamics (CFD) and static structural analysis to investigate the aerodynamic and structural performance of a rigid honeybee-inspired wing. The methodology is divided into several stages, as described below [3][2].



#### 4.1. Geometry Preparation

The wing geometry is designed based on the morphology of the honeybee species *Apis mellifera* to serve as a rigid, non-deforming wing for aerodynamic and structural analysis. The geometry is created using CAD software (SolidWorks), following the general planform shape of a honeybee wing, including approximate span, chord, and aspect ratio based on biological data. As the study focuses on rigid wing performance, geometric simplifications are made by excluding fine structural details such as venation, flexibility, and membrane properties [6][7]. The finalized geometry is then exported in a compatible format and imported into ANSYS for meshing and simulation. In CFD simulations, the wing remains fixed within the computational domain, and different phases of flapping motion are approximated by altering the direction of incoming airflow to simulate discrete angles of attack, rather than physically rotating the wing. For structural analysis, the same rigid geometry is used, with the wing root fixed to simulate attachment to the drone body. Pressure loads from CFD are then applied to evaluate deformation and stress [7].

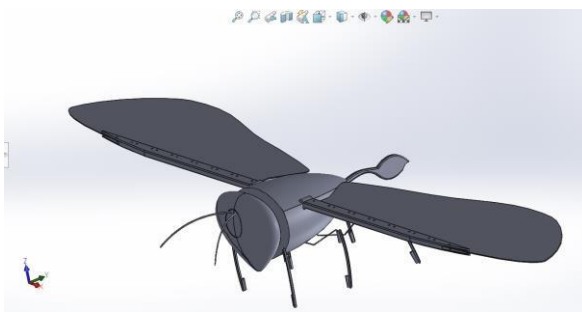


**Figure 4.1-1 Geometry (SolidWorks)**

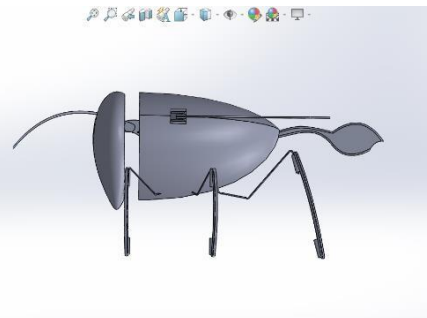


**Figure 4.1-2 Geometry Side view**

#### 4.2. Computational Domain Creation

A sufficiently large fluid domain is constructed around the wing geometry to ensure that boundary effects do not interfere with flow development. The domain size is typically set to at least 5–10 times the chord length of the wing in all directions, allowing the full development of flow structures such as vortices and wake patterns. The wing is positioned at the center of the domain, with the root fixed at the origin.

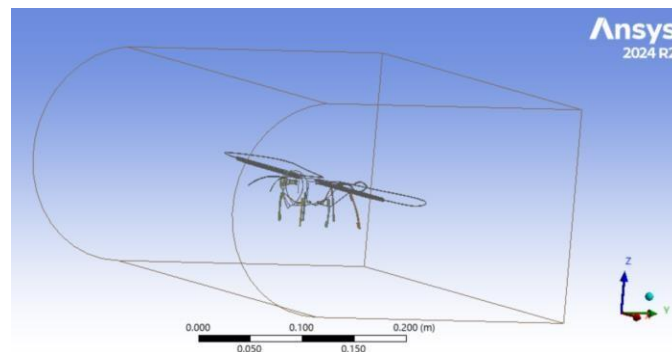


**Figure 4.2 Domain set up in Ansys design modular**

#### 4.3. Meshing

The domain and wing geometry are discretized using a high-quality mesh generated in ANSYS Meshing. The mesh generation process includes the following considerations:

- Mesh type: Unstructured tetrahedral mesh with inflation layers near the wing surface to capture boundary layer effects.
- Inflation layers: 10–15 layers with a smooth growth rate to resolve near-wall gradients [7][1][8].
- Curvature and proximity control: Applied to accurately capture fine features near leading edges and wing tips.

A mesh independence study is conducted by systematically refining the mesh (coarse, medium, fine) and comparing key aerodynamic outputs (lift and drag) to ensure convergence. The optimal mesh is selected where further refinement results in negligible change in simulation results.

#### Typical Starting Mesh Parameters

- Global element size: ~1–2 mm
- Minimum size near surface: ~0.2 mm
- Growth rate: ~1.2

Case	Mesh Density	Near-Wall Elements	Total Elements
<b>Coarse</b>	Low	~6 inflation layers	~0.5-1 million
<b>Medium</b>	Medium	~10 layers	~2-3 million
<b>Fine</b>	Fine	~12-15 layers	~5-8 million

#### 4.3.1 Mesh Independence Study Setup

A mesh independence study is a critical step in validating CFD results—particularly for a rigid honeybee-inspired wing, where intricate aerodynamic features such as leading-edge vortices and wing-body interactions can be highly sensitive to mesh resolution [1][8][3]. The study involves generating coarse, medium, and fine mesh levels and comparing aerodynamic outputs. The results indicate that fine meshing provides the most accurate solution, with approximately 34 million elements and 6 million nodes.

##### 4.3.1.1. Coarse Meshing:

The result for the coarse meshing is as follows:

<b>Advanced</b>	
Number of CPUs for Parallel Part Meshing	Program Controlled
Straight Sided Elements	
Rigid Body Behavior	Dimensionally Reduced
Triangle Surface Mesher	Program Controlled
Topology Checking	Yes
Pinch Tolerance	Default (1.8e-004 m)
Generate Pinch on Refresh	No
<b>Statistics</b>	
<input type="checkbox"/> Nodes	631259
<input type="checkbox"/> Elements	3463598
Show Detailed Statistics	No

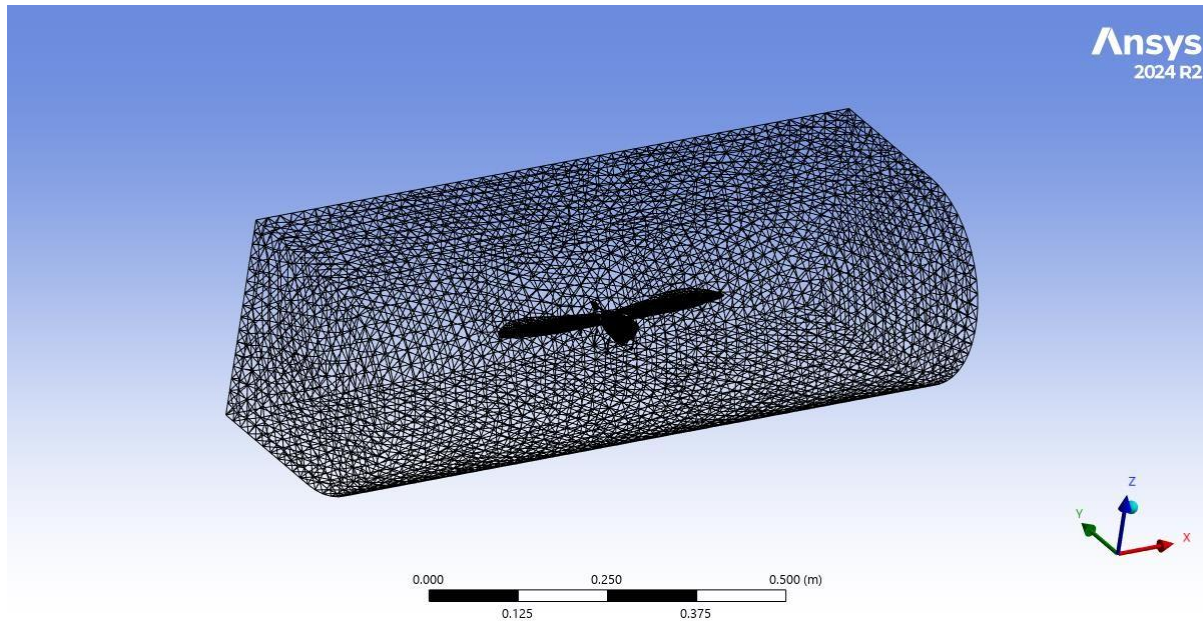


**Figure 4.3.1-1 Coarse Meshing View 1**

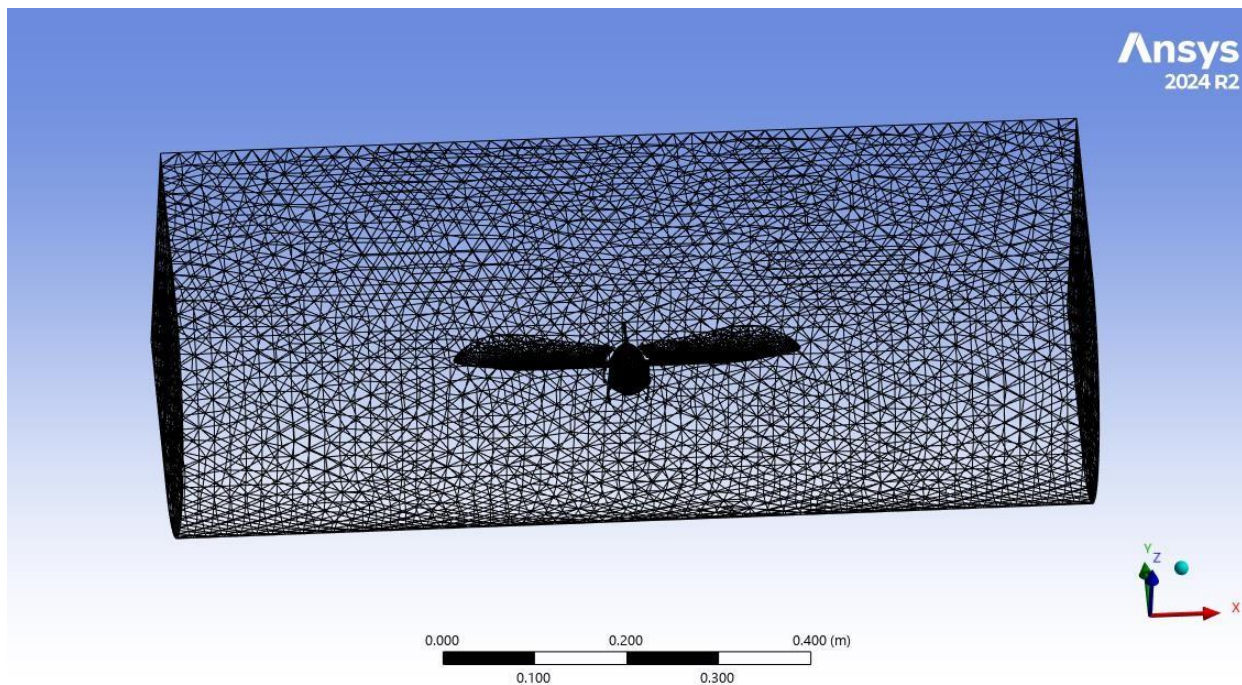


**Figure 4.3.1-0-1 Coarse Meshing View 2**

**4.3.1.2. Medium Meshing:** The results for medium meshing are as follows:

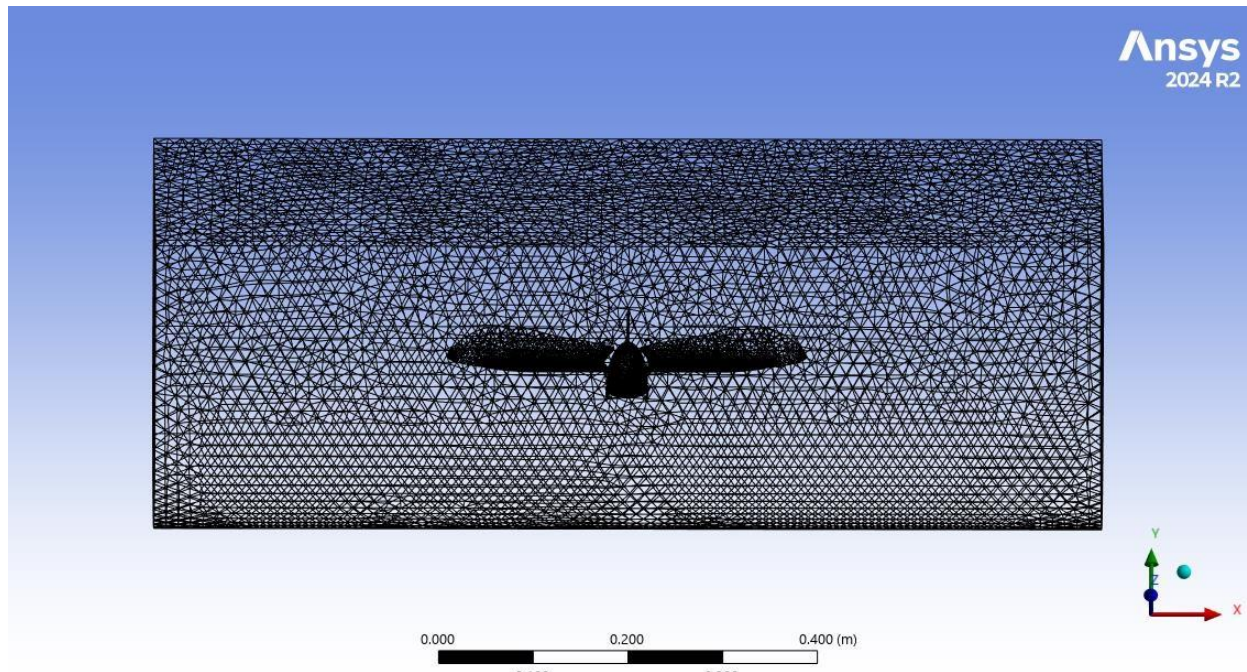


**Figure 4.3.1-2 Medium Meshing View 1**

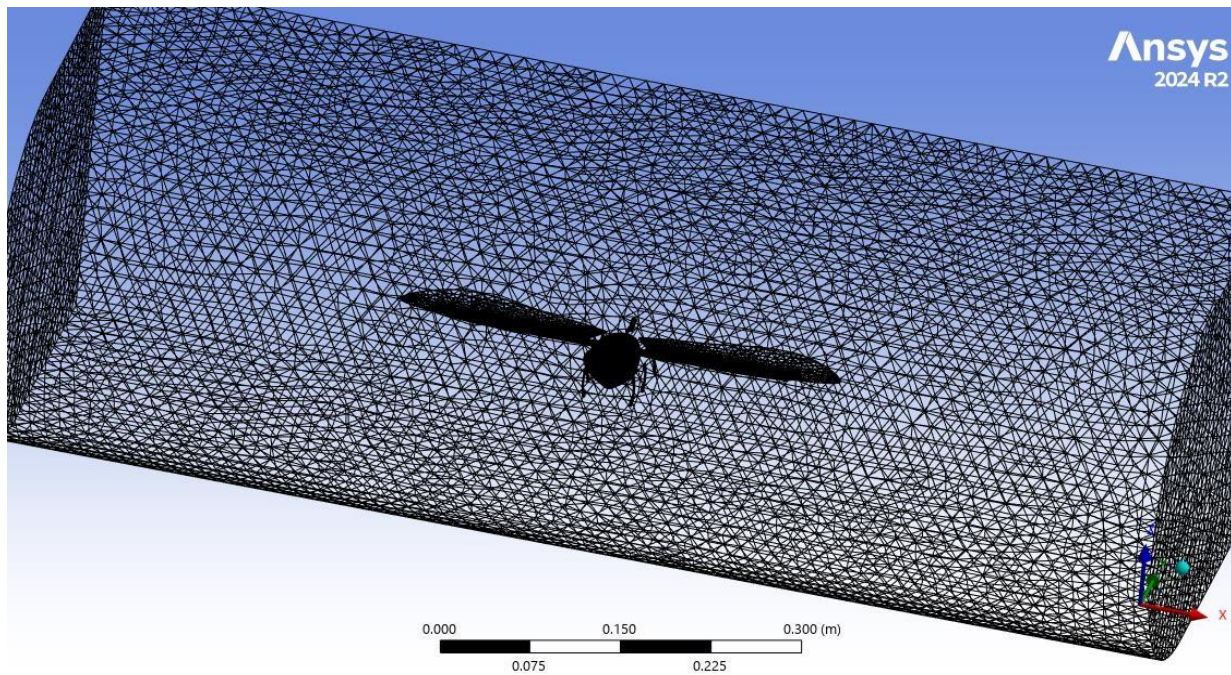


**Figure 4.3.1-2 Medium Meshing View 2**

#### 4.3.1.3 Fine Meshing:

The best Results were shown by Fine level of meshing which has the following results:

Advanced	
Number of CPUs for Parallel Part Meshing	Program Controlled
Straight Sided Elements	
Rigid Body Behavior	Dimensionally Reduced
Triangle Surface Mesher	Program Controlled
Topology Checking	Yes
Pinch Tolerance	Default (1.8e-005 m)
Generate Pinch on Refresh	No
Statistics	
Nodes	6237999
Elements	34914793
Show Detailed Statistics	No

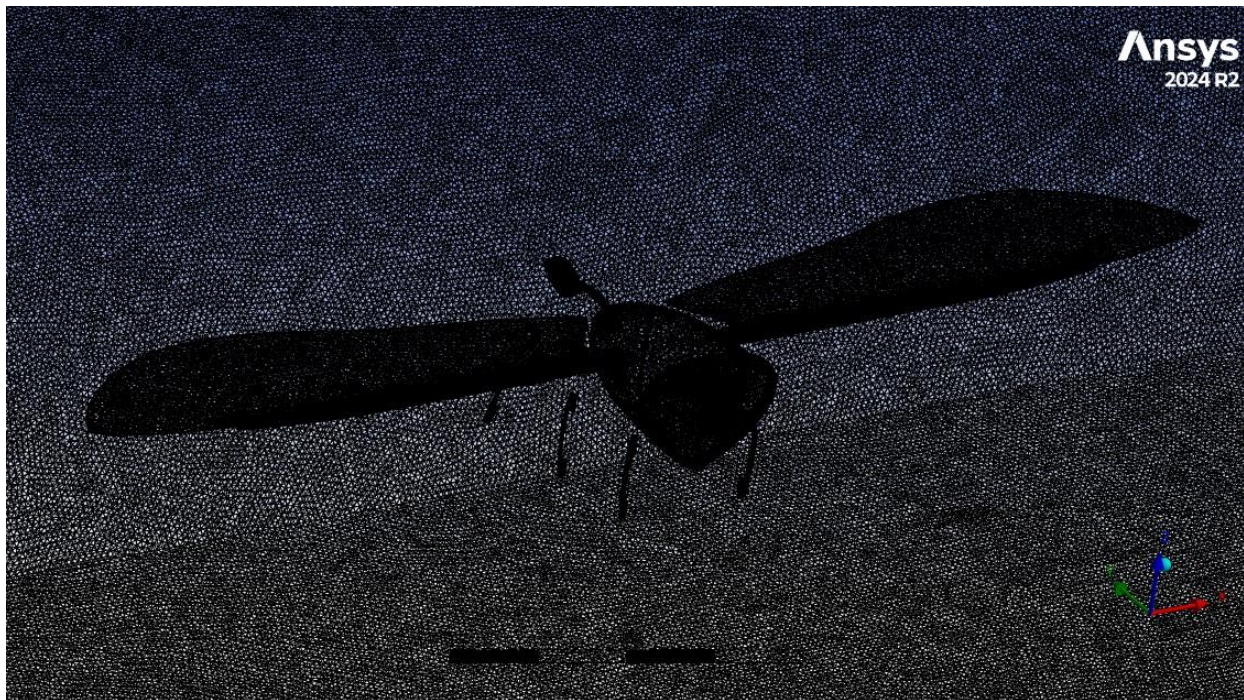


**Figure 4.3.1-3 Fine Meshing View**

#### 4.4 CFD Simulation Setup (ANSYS Fluent)

The Computational Fluid Dynamics (CFD) analysis for the honeybee-inspired rigid wing is performed using ANSYS Fluent. A pressure-based, steady-state solver is employed, which is suitable for the low-speed, incompressible flow regime typical of micro aerial vehicles operating in hover or low forward flight conditions. The simulations are conducted at three different angles of attack (AoA) to evaluate lift and drag forces. These simulations also provide pressure contour data during post-processing [8][9]. The following parameters are used for the CFD setup:

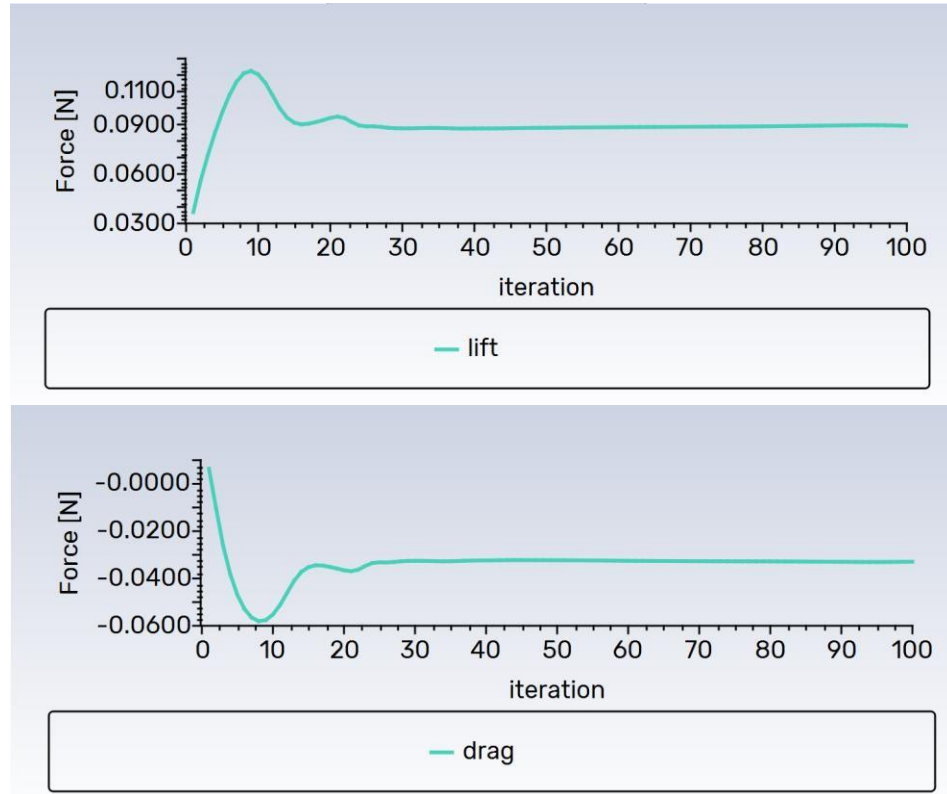
**Table 4.4 – Flow Parameters**

Parameter	Value
<b>P (density)</b>	1.225 kg/m <sup>3</sup>
<b>V (velocity)</b>	5 m/s
<b>A (Area)</b>	0.001895 m <sup>2</sup>

Since the drone's default geometry lies in the YZ plane, velocity components are adjusted accordingly for each AoA:

**Table 4.4.1 – Velocity Components for Different AoA**

AoA	V (m/s)	Vy (m/s)	Vz (m/s)
30°	5	4.3301	2.5
40°	5	3.8302	3.2139
45°	5	3.5355	3.5355

**Lift and Drag Plot at 30 AoA:**

Console	
Force	[N]
-----	-----
wall-air	0.089189894
Force	[N]
-----	-----
wall-air	-0.032911129

**Figure 4.4 Lift and Drag Plots for 30 AoA**

**Observation:** Lift and drag did not converge at 50° AoA because it corresponds to the stall condition for the honeybee-inspired wing, which aligns with biological data indicating a maximum AoA of ~50° for natural honeybee wings [7].

## Lift Plot at 40 AoA:

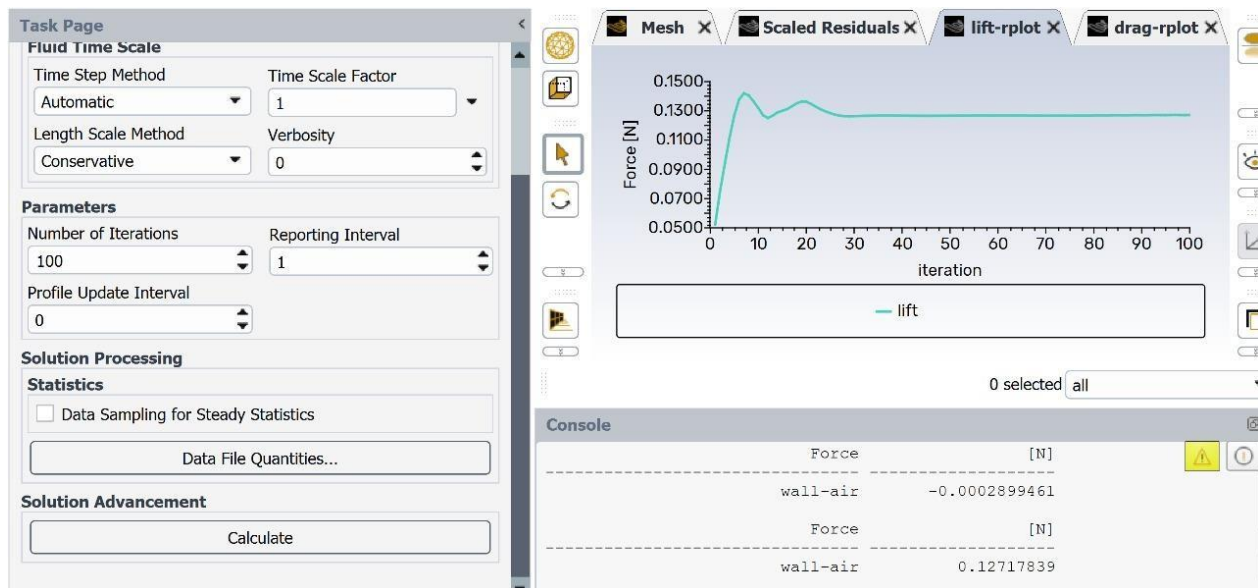


Figure 4.4 Lift Plot for 40 AoA

## 4.5. Post-Processing

After completing the CFD simulations in ANSYS Fluent, the following post-processing steps were performed:

### 4.5.1. Aerodynamic Post-Processing

- **Force Calculations:** Aerodynamic forces (Lift, Drag, and Thrust) acting on the wing were extracted using built-in force monitors for each static position and flow condition.
- **Pressure and Velocity Contours:** Contour plots of pressure and velocity were generated to visualize flow behavior, particularly near the leading edge and wingtip regions [3][4][9].
- **Vorticity and Vortex Visualization:** Vortex structures, including Leading-Edge Vortices (LEV) and wingtip vortices, were visualized using vorticity magnitude plots and Q-criterion iso-surfaces to assess their contribution to lift and thrust generation [8][7].
- **Flow Separation Analysis:** Regions of flow separation and stall were identified at higher AoA, providing insight into unsteady aerodynamic behavior.
- **Lift-to-Drag Ratio Evaluation:** Aerodynamic efficiency was assessed by calculating L/D ratios at different angles of attack.

### 4.5.2. Pressure Contours

The pressure contour analysis for 30° and 40° AoA reveals significant differences:

- At 30° AoA, low-pressure regions on the upper surface indicate strong suction and stable LEV behavior.
- At 40° AoA, a pronounced suction peak forms, but a large flow separation region emerges, signaling the onset of stall [6][9].

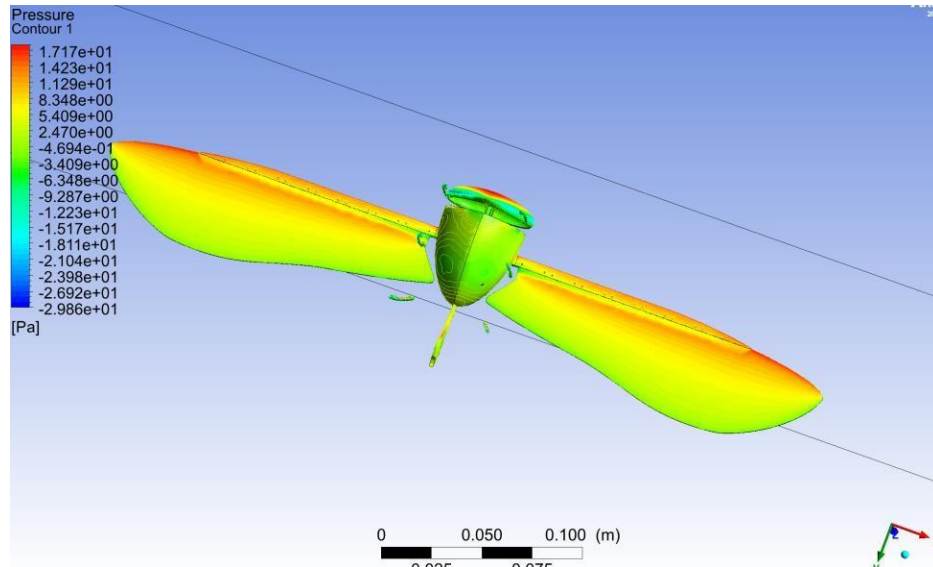


**Figure 4.5.2 Pressure Contours at 30 AoA**

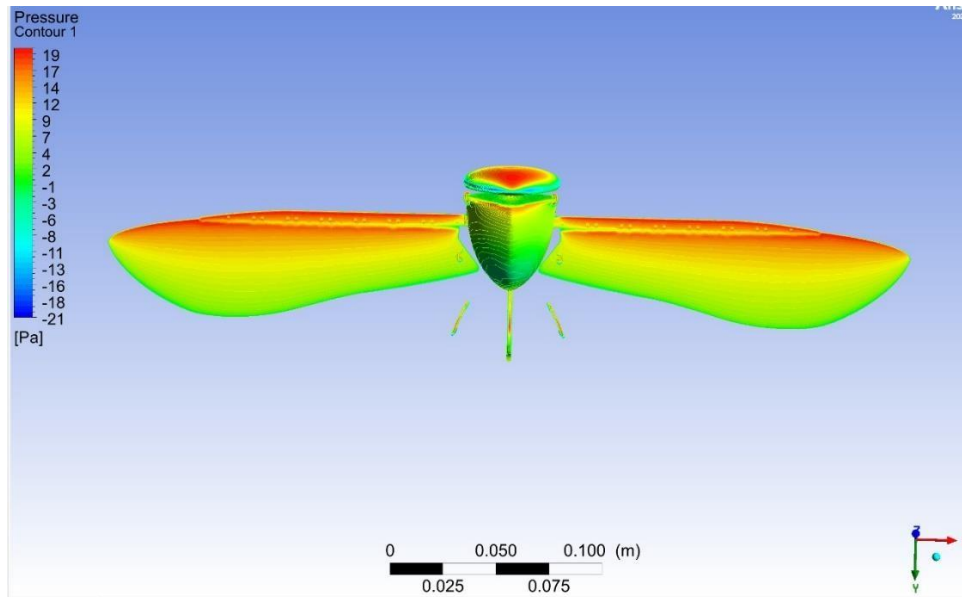


**Figure 4.5.2 Pressure contours at 40 AoA**

### 4.5.3. Velocity Contours

Key observations from velocity contour analysis:

#### At 30° AoA:

- Accelerated flow over the upper surface, especially near the leading edge, indicates strong suction and lift.
- LEV remains attached, energizing the boundary layer and delaying separation [7][5].
- Wake is narrow and streamlined, suggesting efficient momentum recovery.

#### At 40° AoA:

- Sharp velocity drop along the upper surface mid-chord, indicating early separation.
- LEV breakdown occurs, reducing aerodynamic efficiency.
- Broad wake region with recirculation zones—typical stall characteristics [3][7].

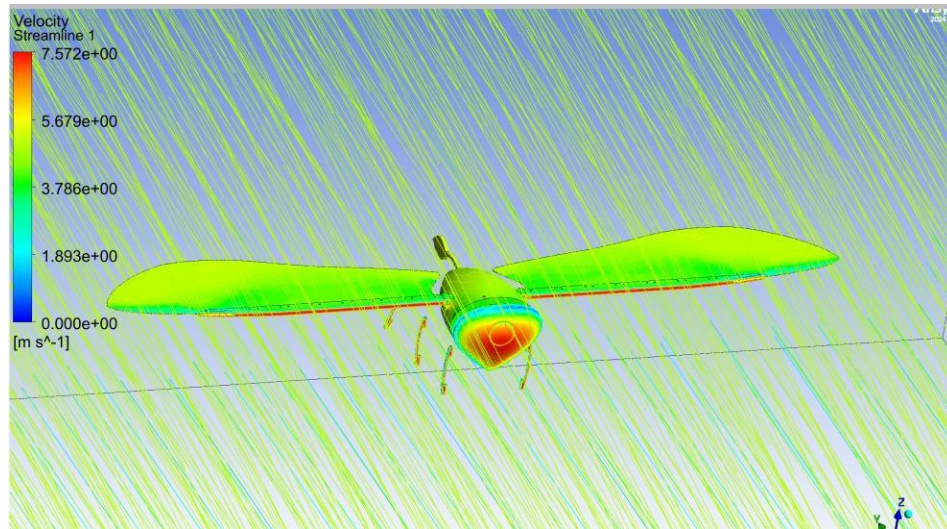


Figure 4.5.3 Velocity Contours at 30 AoA

#### 4.5.4. yPlus Value

The  $y^+$  values for all cases are less than 1, indicating an adequately fine near-wall mesh suitable for the selected turbulence model. This ensures accurate prediction of boundary layer phenomena such as wall shear stress and flow separation [6][9].

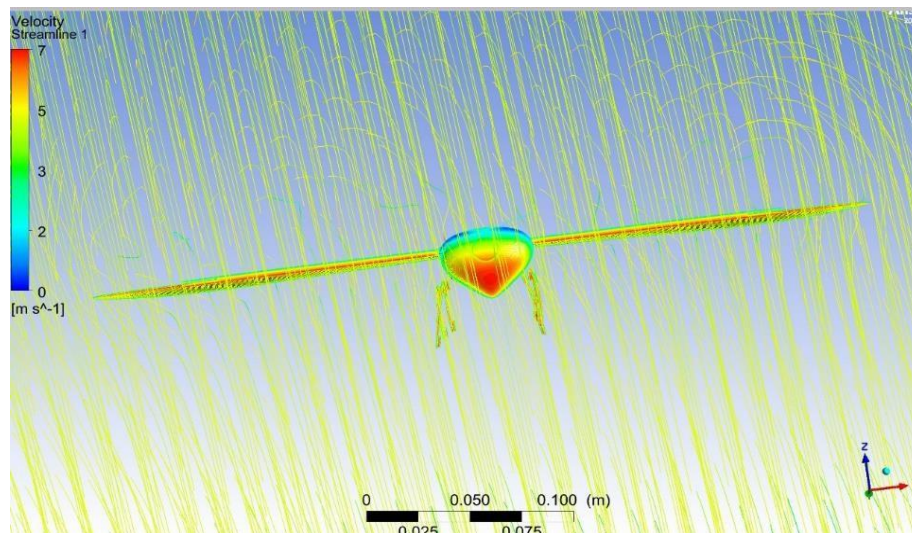


Figure 4.5.3 Velocity Contours at 40 AoA

## 5. Conclusion

This study validates the aerodynamic and structural feasibility of a rigid honeybee-inspired wing for micro-aerial vehicle (MAV) applications. The findings underscore the potential of biomimetic design, demonstrating that even a simplified, rigid interpretation of complex biological wing mechanics can yield aerodynamically efficient and structurally robust designs. Future work will explore dynamic flapping mechanisms, incorporate flexible wing models, and include unsteady simulations to capture time-dependent effects more accurately. Additionally, environmental factors such as wind gusts and turbulence will be considered to further optimize the design. Ultimately, this research lays the groundwork for developing highly agile and efficient bio-inspired drones for diverse applications [10].

## 9. References

- [1] Badrya, C., Govindarajan, B., Baeder, J., Harrington, A., & Kroninger, C. (2019). Computational and experimental investigation of a flapping-wing micro air vehicle in hover. *Journal of Aircraft*, 56(4), 1610–1625. <https://doi.org/10.2514/1.C035340>
- [2] Bohorquez, F., Samuel, P., & Waszak, M. (2003). Design, analysis and hover performance of a rotary wing micro air vehicle. *Journal of the American Helicopter Society*, 48(2), 80–90. <https://doi.org/10.4050/JAHS.48.80>
- [3] Bolsman, G., & Van Keulen, F. (2009). Design overview of a resonant wing actuation mechanism for application in flapping wing MAVs. *International Journal of Micro Air Vehicles*, 1(4), 263–272. <https://doi.org/10.1260/175682909789498380>
- [4] Aono, H., & Liu, H. (2008). A numerical study of hovering aerodynamics in flapping insect flight. In N. Kato & S. Kamimura (Eds.), *Bio-mechanisms of swimming and flying* (pp. 179–191). Springer. [https://doi.org/10.1007/978-4-431-78158-3\\_16](https://doi.org/10.1007/978-4-431-78158-3_16)
- [5] Aono, H., Liang, F., & Liu, H. (2008). Near- and far-field aerodynamics in insect hovering flight: An integrated computational study. *Journal of Experimental Biology*, 211(2), 239–257. <https://doi.org/10.1242/jeb.012401>
- [6] Bai, P., Cui, E., Li, F., Zhou, W., & Chen, B. Y. (2007). A new bionic MAV's flapping motion based on fruit fly hovering at low Reynolds number. *Acta Mechanica Sinica*, 23(5), 485–493. <https://doi.org/10.1007/s10409-007-0104-4>
- [7] Feaster, J., Battaglia, F., & Bayandor, J. (2017). A computational study on the influence of insect wing geometry on bee flight mechanics. *Biology Open*, 6(12), 1784–1795. <https://doi.org/10.1242/bio.024612>
- [8] McBride, D. (2007). A coupled finite volume method for the solution of flow processes on complex geometries. *International Journal for Numerical Methods in Fluids*, 54(2), 173–197. <https://doi.org/10.1002/fld.1405>
- [9] Hamdani, S. H. R., Zehra, F. T., & Sohail, M. U. (2025). Design of corrugated airfoil for a flapping wing micro air vehicle. *International Journal of Aerospace Engineering*, 2025, Article ID 8837246. <https://doi.org/10.1155/2025/8837246>
- [10] Rees, C. J. C. (1975). Aerodynamic properties of an insect wing section and a smooth aerofoil compared. *Nature*, 258(5531), 141–142. <https://doi.org/10.1038/258141a0>
- [11] Haider, N., Shahzad, A., Mumtaz Qadri, M. N., & Ali Shah, S. I. (2021). Recent progress in flapping wings for micro aerial vehicle applications. *Chinese Journal of Aeronautics*, 34(3), 1–18. <https://doi.org/10.1016/j.cja.2020.10.031>

## 10. Conflict of Interest

The authors declare that there are no conflicts of interest to report this article.

## 11. Funding

No external funding was received to support this study.